A General Dynamic Model for Multiphase Electrolytic Systems

C. Coussine, J.-P. Serin, P. Cézac, F. Contamine and J.-M. Reneaume
Univ Pau & Pays Adour, LaTEP EA 1932 - Laboratoire de Thermique, Energétique et Procédés, ENSGTI - Rue Jules Ferry, BP 7511 Pau, F-64075, France

C. Coussine, K. Dubourg, A. Knorst and J. Cambar
Institut du thermalisme, Université Victor Segalen Bordeaux 2, 8 rue Sainte Ursule, 40100 Dax, France

DOI 10.1002/aic.13758
Published online February 24, 2012 in Wiley Online Library (wileyonlinelibrary.com).

The study and characterization of aqueous solutions are becoming an important research topic because of their central role in many processes. The modeling of these solutions is complicated by different factors: the important number of ionic and nonionic species, the nonideality of aqueous solutions, the appearance and disappearance of thermodynamic phases (solid, vapor) depending on operating conditions. This article presents a general model in dynamic state of aqueous electrolytic system involving liquid, vapor, and solid phases. The mathematical formulation includes: physical and chemical equilibria, mass and energy balances, electroneutrality equation and evaporation equation. The set of equations is solved by the Gear's method. The model is validated by the comparison between modeled results (activity coefficients, solubility, evaporite sequence) and experimental data. One of the purposes of the model will be the simulation of a production process of salt crystals and waters concentrated in minerals of interest. © 2012 American Institute of Chemical Engineers *AIChE J,* 58: 3832–3840, 2012

Keywords: thermodynamics, electrolytes, modeling, dynamic, salts

Introduction

Aqueous solutions are involved in many processes: seawater desalination, crystallization, corrosion studies, hydrometallurgical studies, and environmental applications like wastewater treatment or gas treatment. Many factors must be taken into account for the modeling of aqueous solutions: the large number of ionic and neutral species, the strong nonideality of solutions due to the presence of electrolytes, the appearance and disappearance of solid phases. So, the study of aqueous solutions continues to be an important research topic.

The aim of this study is to propose a general model to simulate a multiphase electrolytic system in dynamic state. The process simulated is a perfectly agitated batch reactor, in which aqueous solution is heated. The solution is concentrated by evaporation of water. One of the model purposes is the simulation of a production process of salt crystals and waters concentrated in minerals of interest for health using natural salt waters. The characteristics and species of salt waters are similar to the seawater properties but each salt water composition is different.

In this article, the model is described and the results obtained for seawater and artificial salt water are presented. The proposed model aims to be a practical engineer tool.

Correspondence concerning this article should be addressed to C. Coussine at charlotte.coussine@univ-pau.fr.

Model Description

The developed general triphasic model is based on a thermodynamic description of the macroscopic physical–chemical phenomena occurring in a gas–liquid–solid system, which is assumed perfectly mixed at a temperature below the boiling point. Our model can accurately predict the resulting phase distribution and phase composition in dynamic state for electrolytic batch reactor. Figure 1 shows the schematic process.

Governing equations

The governing equations are Carrier's correlation (evaporation equation), equilibrium equations and balances (mass balances, charge balance, and energy balance).

Carrier's Correlation. The evaporation flow is calculated through the Carrier's correlation. This correlation is the most published and used for the determination of water evaporation rate.[1] It depends on the background of the process (velocity and water amount of the air below the vessel), the process device (evaporation area of the reactor), and thermodynamic properties (latent heat of vaporization of compounds, liquid–gas equilibrium).

$$V - (0.089 + 0.40782.\mathrm{vel}).A.\sum_{i=1}^{n\mathrm{vapor}} \frac{y_i P - y_{a_i}.P}{\Delta H_{LV_i}(T)} = 0 \qquad (1)$$

where vel and y_{ai} are characteristics of the air below the reactor (velocity in m s^{-1} and vapor molar fraction of compound i), A is the evaporation area of the vessel (in m^2), y_i is the vapor molar fraction of compound i at the equilibrium

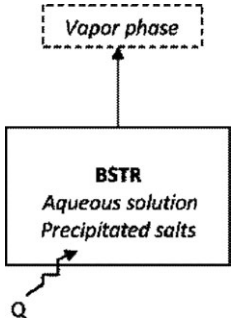

Figure 1. Schematic diagram.

(–), P is the pressure (in Pa), T is the temperature (in K), and ΔH_{LV} is the latent heat of vaporization (in J mol^{-1}).

Physical and Chemical Equilibria. Two types of equilibria have to be considered: chemical and physical equilibria. The chemical potential is the criterion of the equilibrium.

Chemical equilibria. In aqueous solutions, solutes dissociate to form anions and cations.

$$C_{\nu_C}A_{\nu_{A(aq)}} \leftrightarrow \nu_A A_{(aq)} + \nu_C C_{(aq)}$$

where A and C are respectively the anion and cation and $C_{\nu c}A_{\nu a(aq)}$ is the neutral species.

The mathematical equations related to dissociation equilibria are

$$\prod_{i=1}^{n\text{species}} a_i^{\nu_{i,j}} - mK_j^{\text{dis}}(T) = 0 \tag{2}$$

where a_i is the activity of compound i (–),$\nu_{i,j}$ is the stoichiometric coefficient of species i in equilibrium j (–), mK_j^{dis} is the thermodynamic constant of dissociation equilibrium j (–), and T is the temperature (in K).

Physical equilibria. The physical equilibria are basically equilibria between gas and liquid phases and between liquid and solid phases.

Solid–liquid equilibria. The solid–liquid equilibria are written as

$$\nu_A A_{(aq)} + \nu_C C_{(aq)} + \nu_{H_2O} H_2O_{(aq)} \leftrightarrow C_{\nu_C}A_{\nu_A}, \nu_{H_2O}H_2O_{(s)}$$

where A and C are, respectively, the anion and cation and $C_{\nu c}A_{\nu a}, \nu_{H_2O}H_2O_{(s)}$ is the solid.

The mathematical equations related to solid–liquid equilibria are

$$\prod_{i=1}^{n\text{species}} a_i^{\nu_{i,j}} - mK_j^{\text{ELS}}(T) = 0 \tag{3}$$

where a_i is the activity of compound i (–), $\nu_{i,j}$ is the stoichiometric coefficient of species i in equilibrium j (–), mK_j^{ELS} is the thermodynamic constant of solid–liquid equilibrium j (–), and T is the temperature (in K).

Each solid phase is supposed to be pure and its activity equal to 1.

Vapor–liquid equilibria. The unsymmetrical convention is applied. So, the liquid–vapor expressions are different for the water and the solutes. The vapor phase is assumed to be ideal and the Poynting factor is neglected. For the water, the liquid-vapor expression is

$$a_w \cdot P_i^{\text{sat}}(T) = y_w \cdot P \tag{4}$$

where a_w is the water activity (–), P_i^{sat} is the vapor pressure of water (in Pa), y_w is the vapor molar fraction of water (–), and P is the pressure (in Pa). For the solutes, the liquid-vapor expression is

$$m_i.\gamma_i^m(T,P).H_i^m(T,P) = y_i.P \tag{5}$$

where m_i is the molality of compound i (in mol kg^{-1} H_2O), γ_i^m is the activity coefficient on a molal basis (–), and H_i^m is the Henry's law constant on a molal basis (in Pa kg H_2O mol^{-1}).

Balances. We use equations of global mass balance, partial mass balances, charge balance, and energy balance.

Mass balances. The global mass balance is written as

$$\frac{dU}{dt} + V + \sum_{i=1}^{n\text{solids}} \frac{dn_i}{dt} = 0 \tag{6}$$

where U is the charge (in mol), t is the time (in s), V is the evaporation flow (in mol s^{-1}) and n_i is the molar quantity of compound i (in mol).

Partial mass balances can be made on ions or on atoms. We choose to work with partial mass balances on atoms

$$\sum_{i=1}^{n\text{species}} b_i^j \left(U.\frac{dx_i}{dt} + x_i\frac{dU}{dt} + \frac{y_i}{\sum_{i=1}^{n\text{vapor}} y_i}.V \right) + \sum_{i=1}^{n\text{solids}} b_i^j.\frac{dn_i}{dt} = 0 \tag{7}$$

where b_i^j is the number of atom j in species i (–), x_i is the molar fraction of compound i in liquid phase (–) and y_i is the molar fraction of compound i in gas phase (–).

Charge balance. The principle of electroneutrality leads to the following relation

$$\sum_{i=1}^{n\text{ions}} z_i.m_i = 0 \tag{8}$$

where z_i is the ionic charge (–) and m_i is the molality of compound i (in mol kg^{-1} H_2O).

We choose to eliminate one partial mass balance and include the electroneutrality equation.

Energy balance. The energy balance is expressed as

$$U.\frac{dh_l}{dt} + h_l.\frac{dU}{dt} + \sum_{i=1}^{n\text{solids}} n_i.\frac{dh_{ci}}{dt} + h_{ci}.\frac{dn_i}{dt} + V.H_v - Q = 0 \tag{9}$$

where h_l, h_{ci}, and H_v are liquid, solid (crystal), and vapor enthalpies (in J mol^{-1}), respectively and Q is heat (in W).

Table 1. Variables of the Model

Variable	Designation
T	Temperature
Q	Heat
U	Molar quantity of liquid
V	Evaporation flow
x	Molar fractions (liquid phase)
n	Molar quantities of solids
y	Molar fractions (gas phase)

Table 2. Equations of the Model

	Equations
Global mass balance	$\frac{dU}{dt} + V + \sum_{i=1}^{n\text{solids}} \frac{dn_i}{dt} = 0$
Partial mass balances on the atoms	$\sum_{i=1}^{n\text{species}} b_i^{\text{j}} \left(U.\frac{dx_i}{dt} + x_i \frac{dU}{dt} + \frac{y_i}{\sum_{i=1}^{n\text{vapor}} y_i}.V \right) + \sum_{i=1}^{n\text{solids}} b_i^{\text{j}}.\frac{dn_i}{dt} = 0$
Chemical equilibria	$\prod_{i=1}^{n\text{species}} a_{\text{i}}^{\nu_{\text{i,j}}} - mK_{\text{j}}^{\text{dis}}(\text{T}) = 0$
Liquid–solid equilibria	$\prod_{i=1}^{n\text{species}} a_{\text{i}}^{\nu_{\text{i,j}}} - mK_{\text{j}}^{\text{ELS}}(T) = 0$
Liquid–vapor equilibria	$y_{\text{i}} \cdot \Phi_{\text{i}}^{\text{V}}(T,P,y) \cdot P - x_{\text{i}} \cdot \gamma_{\text{i}}(T,P,x) \cdot f_{\text{i}}^{0\text{L}}(T,P) = 0$
Electroneutrality	$\sum_{i=1}^{n\text{ions}} z_i.m_i = 0$
Evaporation flow	$V - (0.089 + 0.40782.\text{vel}).\text{A}.\sum_{i=1}^{n\text{vapor}} \frac{y_{\text{i}}P - y_{\text{a}_{\text{i}}}.P}{\Delta H_{\text{LV}_{\text{i}}}(T)} = 0$
Energy balance	$U.\frac{dh_1}{dt} + h_1.\frac{dU}{dt} + \sum_{\text{i}=1}^{n\text{solids}} n_i.\frac{dh_{\text{ci}}}{dt} + h_{\text{ci}}.\frac{dn_i}{dt} + V.H_v - Q = 0$

Summary of variables and equations

Variables. The variables of the model are presented in Table 1.

Equations. The equations of the model are presented in Table 2.

Numerical Procedure. The set of equations of the proposed model composes a nonlinear differential system, in which all the thermodynamic properties are expressed as functions of state variables (composition, temperature, and pressure). The differential-algebraic equations system is solved by the Gear's method.[2] This method is based on a predictor–corrector scheme with variable order and variable step size.

Thermodynamic Models

Activity coefficients

Different models consider long-range and short-range interactions and can be used to estimate activity coefficients in complex aqueous solutions. Many authors studied these models. For instance, Liddell[3] or more recently Ben Gaïda et al.[4] carried out a survey on these thermodynamic models.

Activity coefficient models for electrolytic solutions are mainly variations of the Debye–Hückel equation taking account of the long-range interaction contribution. The principle of this theory is that the ions contained in a dilute electrolytic solution are considered as punctual charges. So, oppositely charged ions attract one another and like-charged ions repel each other.[5]

Many authors used local composition models adding a Debye–Hückel term to take into account of electrostatic interactions. Kikic et al.[6] have published the first electrolyte model based on a group-contribution method (UNIFAC), in which the electrolytic solution is considered to be a mixture of functional groups (basic building blocks). Chen et al.[7] and Lu et al.[8] extended, respectively, the NRTL and UNIQUAC local composition models to electrolyte solutions. Nicolaisen et al.[9] published results obtained with UNIQUAC electrolyte model and Zemaitis et al.[10] detailed and worked on Chen's model (NRTL electrolyte) for salt solutions. Achard et al.[11] developed the ULPDHS model based on UNIFAC model for the short-range interaction coupled with a Debye-Hückel term to take account of the long-range interaction; hydration of ions or nondissociated molecules is considered via a hydration number. Gros and Dussap[12] studied ULPDHS model.

Another class of models exists. It is based on Debye–Hückel theory, for example, Meissner and Tester,[13] Bromley.[14] In 1973, Pitzer[15] completed the Debye–Hückel equation with a virial expansion to take account of short-range interactions. The Pitzer's activity coefficient model is the most popular in geochemistry for the characterization of salt water like seawater and

Table 3. Binary Parameters' Pitzer at 298.15 K and 1 atm

	β_0	β_1	C^Φ	β_0	β_1	C^Φ	β_0	β_1	C^Φ	β_2
		OH^-			Cl^-			SO_4^{2-}		
Na^+	8.63d-2[a]	0.253[a]	4.10d-3[a]	7.54d-2[b]	0.277[b]	1.37.d-3[b]	1.27d-2[c]	1.09[c]	6.27d-3[c]	–
K^+	0.130[i]	0.320[i]	4.10d-3[i]	4.81d-2[j]	0.219[j]	−7.88.d-4[j]	3.80d-3[k]	1.05[k]	1.48d-2[k]	–
Mg^{2+}	–	–	–	0.351[l]	1.65[l]	6.51.d-3[l]	0.215[a]	3.37[a]	2.79d-2[a]	−32.8[a]
H^+	–	–	–	0.177[m]	0.297[m]	3.62.d-4[m]	7.07d-2[n,o]	9.71d-3[n,o]	−0.313[n,o]	–
Ca^{2+}	–	–	–	0.305[p]	1.71[p]	2.34.d-3[p]	0.115[k]	3.56[k]	3.98d-2[k]	−61.7[k]

	β_0	β_1	C^Φ	β_0	β_1	C^Φ	β_0	β_1	C^Φ	β_0	β_1	C^Φ
		HCO_3^-			CO_3^{2-}			Br^-			F^-	
Na^+	2.80d-2[d]	4.40d-2[d]	–	3.62d-2[e]	1.51[e]	5.20d-3[e]	9.73d-2[f,g,h]	0.279[f,g,h]	1.16d-3[f,g,h]	0.215[f,g,h]	0.211[f,g,h]	–
K^+	−1.07d-2[d]	4.78d-2[d]	–	0.129[d]	1.43[d]	5.00d-4[d]	5.69d-2[f,g,h]	0.212[f,g,h]	−1.80d-3[f,g,h]	8.09d-2[f,g,h]	0.202[f,g,h]	9.30d-4[f,g,h]
Mg^{2+}	−9.31d-3[d]	0.805[d]	–	–	–	–	0.433[g,h]	1.75[g,h]	3.12d-3[g,h]	–	–	–
H^+	–	–	–	–	–	–	0.196[f,g,h]	0.356[f,g,h]	8.27d-3[f,g,h]	–	–	–
Ca^{2+}	0.183[d]	0.300[d]	–	–	–	–	0.382[g,h]	1.61[g,h]	−2.57d-3[g,h]	–	–	–

[a]From Pabalan and Pitzer.[18]
[b]From Pitzer et al.[19]
[c]From Spencer et al.[20]
[d]From He and Morse.[21]
[e]From Peiper and Pitzer.[22]
[f]From Silvester and Pitzer[23]
[g]From Criss and Millero.[24]
[h]From Pitzer and Mayorga.[25]
[i]From Millero and Pierrot.[16]
[j]From Holmes and Mesmer.[26]
[k]From Marion and Farren.[27]
[l]From De Lima and Pitzer.[28]
[m]From Holmes et al.[29]
[n]From Pierrot et al.[30]
[o]From Campbell et al.[31]
[p]From Moller.[32]
Parameters not presented or with the symbol (–) are assumed null. Most of these parameters are temperature dependant.

Table 4. Mixed Parameters' Pitzer at 298.15K and 1 atm

θ_{cc}					
		K^+	Mg^{2+}	H^+	Ca^{2+}
Na^+		−3.20.d-3[a]	7.00.d-2[b]	3.60d-2[c]	5.00d-2[d]
K^+		–	–	–	5.64d-2[d]
Mg^{2+}		–	–	0.100[c]	0.124[d]
θ_{aa}					
		Cl^-	SO_4^{2-}	HCO_3^-	CO_3^{2-}
OH^-		−5.00d-2[c]	−1.30d-2[c]	–	–
Cl^-		–	–	3.59d-2[e,f]	−5.30d-2[e,f]
HCO_3^-		–	–	–	−4.00d-2[c]
Ψ_{cca}					
		K^+	Mg^{2+}	H^+	Ca^{2+}
Cl^-	Na^+	−3.69d-3[a]	−1.20d-2[b]	–	–
	K^+	–	–	−1.10d-2[d]	−2.86d-2[d]
	Mg^{2+}	–	–	−1.10d-2[c]	–
	H^+	–	–	–	8.00d-4[g]
SO_4^{2-}	Na^+	4.15d-3[h]	−2.33d-2[d]	–	−7.34d-2[h]
	K^+	–	−0.124[h]	0.197[i]	–
HCO_3^-	Na^+	−7.90d-3[i]	–	–	–
Ψ_{aac}					
		Cl^-	SO_4^{2-}	HCO_3^-	CO_3^{2-}
Na^+	OH^-	–	−9.00d-3[c]	–	–
	Cl^-	–	−4.81d-3[d]	−1.43d-2[f,j]	1.60d-2[f,j]
	SO_4^{2-}	–	–	−5.00d-3[c]	–
K^+	OH^-	−6.00d-3[c]	−5.00d-2[c]	–	−1.00d-2[h]
	Cl^-	–	−3.83d-3[h]	–	4.00d-3[c]
	SO_4^{2-}	–	–	–	−9.00d-3[c]
Mg^{2+}	Cl^-	–	−0.136[h]	−9.60d-2[h]	–
Ca^{2+}	Cl^-	–	−5.44d-2[h]	–	–

[a]From Greenberg and Moller.[33]
[b]From Pabalan and Pitzer.[18]
[c]From Harvie et al.[34]
[d]From Spencer et al.[20]
[e]From Peiper and Pitzer.[22]
[f]From Thurmond and Millero.[35]
[g]From Roy et al.[36]
[h]From Marion and Farren.[27]
[i]From Marion.[37]
[j]From Roy et al.[38]
Parameters not presented or with the symbol (–) are assumed null. Most of these parameters are temperature dependant.

natural or artificial mineral waters, even if its number of parameters is large. In this study, we use this model.

Pitzer model

Equations. The general equations of Pitzer model[16,17] are presented below for the activity coefficient calculation of cations C (Eq. 10), anions A (Eq. 11), and neutral species N (Eq. 12).

$$\ln\gamma_C = z_C^2.F + \sum_{a=1}^{n_a} m_a.[2.B_{Ca} + Z.C_{Ca}] + \sum_{c=1}^{n_c} m_c \cdot\left[2.\Phi_{Cc} + \sum_{a=1}^{n_a} m_a.\Psi_{Cca}\right] + \sum_{a=1}^{n_a}\sum_{a'=1}^{n_{a'}} m_a.m_{a'}.\Psi_{Caa'} + |z_C|.\sum_{c=1}^{n_c}\sum_{a=1}^{n_a} m_c.m_a.C_{ca} \quad (10)$$

$$\ln\gamma_A = z_A^2.F + \sum_{c=1}^{n_c} m_c.[2.B_{cA} + Z.C_{cA}] + \sum_{a=1}^{n_a} m_a \cdot\left[2.\Phi_{Aa} + \sum_{c=1}^{n_c} m_c.\Psi_{cAa}\right] + \sum_{c=1}^{n_c}\sum_{c'=1}^{n_{c'}} m_c.m_{c'}.\Psi_{cc'A} + |z_A|.\sum_{c=1}^{n_c}\sum_{a=1}^{n_a} m_c.m_a.C_{ca} \quad (11)$$

Table 5. Parameters' Pitzer at 298.15K and 1 atm for CO_2 (He and Morse[21])

	λ			ζ	
Cations	Na^+	8.15d-2		Cl^-	SO_4^{2-}
	K^+	4.49d-2	Na^+	−5.72d-4	−3.75d-2
	Mg^{2+}	0.145	K^+	−1.21d-2	−3.58d-4
	Ca^{2+}	0.164	Mg^{2+}	−9.85d-3	−4.16d-2
Anions	Cl^-	2.05d-2	H^+	−4.71d-3	–
	SO_4^{2-}	0.139	Ca^{2+}	−1.41d-2	–

Parameters not presented or with the symbol (–) are assumed null. Most of these parameters are temperature dependant.

$$\ln\gamma_N = \sum_{c=1}^{n_c} 2.m_c.\lambda_{n,c} + \sum_{a=1}^{n_a} 2.m_a.\lambda_{n,a} + \sum_{c=1}^{n_c}\sum_{a=1}^{n_a} m_c.m_a.\zeta_{n,c,a} \quad (12)$$

Z is a function of molalities (m_i) and ionic charges (z_i). Ψ_{ijk} are the interaction parameters between cations, cations and anions or anions, anions and cations. $\lambda_{n,i}$, $\zeta_{n,i,j}$ are interaction parameters between neutral species, anions and cations. F, B_{ij}, C_{ij}, Φ_{ij} are functions of interaction parameters and are detailed in Appendix.

Parameterization. Pitzer model is parameterized from binary and common-ion ternary systems. The adjustable parameters are the single electrolyte parameters cation–anion, the mixing electrolyte parameters cation–cation, anion–anion, cation–cation–anion, and anion–anion–cation, the binary parameters neutral species–cation, neutral species–anion, and the ternary parameters neutral species–cation–anion. Our model can treat the major ions of salt water: sodium, potassium, magnesium, hydrogen, calcium, hydroxide, chloride, sulfate, bicarbonate, carbonate, bromide, fluoride, carbon dioxide, and water. Many authors have previously evaluated the parameters needed for this system. The adjustable

Table 6. Liquid Solid Equilibrium Constants at 298.15K

Solid	Ksp
NaCl	37.2[a]
Na_2SO_4	0.510[b]
$Na_2SO_4{\cdot}10H_2O$	5.99d-2[b]
$NaHCO_3$	0.400[a,c]
$Na_2CO_3{\cdot}10H_2O$	0.157[c]
NaBr	942[d]
$NaBr{\cdot}2H_2O$	127[d]
KCl	7.94[a]
K_2SO_4	1.66d-2[a,e]
$KHCO_3$	1.55[c]
KBr	11.7[d]
$MgCl_2{\cdot}6H_2O$	28,200[a]
$MgSO_4{\cdot}H_2O$	0.656[a]
$MgSO_4{\cdot}6H_2O$	2.36d-2[f]
$MgSO_4{\cdot}7H_2O$	1.31d-2[g]
$CaCl_2{\cdot}6H_2O$	13,800[a]
$CaSO_4$	6.43d-5[h]
$CaSO_4{\cdot}1/2H_2O$	2.18d-4[d]
$CaSO_4{\cdot}2H_2O$	3.29d-5[d]
$CaCO_3$	4.37d-9[a]

Data used come from:
[a]Risacher and Fritz.[39]
[b]Marliacy et al.[17]
[c]Marion.[37]
[d]Johnson et al.[40]
[e]Jimenez et al.[41]
[f]Marion and Farren.[27]
[g]Plummer et al.[42]
[h]Marshall and Slusher.[43]

Table 7. Artificial Seawater Composition[56,57]

Component	Molality (mol kg^{-1} d'H_2O)
NaCl	0.424
$MgCl_2$	0.0553
Na_2SO_4	0.0291
$CaCl_2$	0.0105
KCl	0.0094

parameters are functions of temperature and are available in Refs. [18–38].

The values of the parameters used in this study are presented at 298.15 K in Table 3 for binary parameters, Table 4 for mixing parameters, and Table 5 for neutral species parameters.

Equilibrium constants

The liquid–solid equilibrium constants are classically calculated from standard Gibbs free energy and depend only on temperature

$$K^{\mathrm{ELS}}(T) = \exp\left(\frac{-\Delta G_{\mathrm{R}}^{0}(T)}{R.T}\right) \tag{13}$$

where $\Delta G_R{}^0$ is the standard Gibbs free energy (J mol^{-1}) and R is the gas constant (in J mol^{-1} K^{-1}).

The functions K^{ELS}(T) are available in the references cited in Table 6. The values of liquid–solid equilibrium constants used in this model are presented at 298.15 K in Table 6.

Water vapor pressure

Antoine's law is used

$$\log\ (P_{\mathrm{sat}_{\mathrm{H_2O}}}) = A - \frac{B}{T + C} \tag{14}$$

where $P_{\mathrm{sat}_{\mathrm{H_2O}}}$ is the vapor pressure of water (in bar) and T is the temperature (K). The Antoine coefficients (A, B, and C) come from Stull[44] and are published by the National Institute of Standards and Technology.

Henry's constant

The equation used to calculate Henry's law constant of solute i in water comes from Yaws et al.[45] Parameters are available in their article.

$$\log\ (H_{\mathrm{i_w}}) = A + \frac{B}{T} + C.\log(T) + D.T \tag{15}$$

where H_{iw} is the Henry's law constant of solute i in water (in Pa).

Table 9. Deviations between Experimental and Calculated Activity Coefficients of Seawater

Na^+	Mg^{2+}	Ca^{2+}	K^+	Cl^-	$SO_4{}^{2-}$	NaCl	Na_2SO_4
2.8%	34%	7.5%	3.3%	2.1%	11%	0%	1.3%

Enthalpies

The enthalpy of solution is calculated as the sum of ideal enthalpy and excess enthalpy. The reference enthalpies for the solutes are considered as formation enthalpies.[10] The data used to determine ideal enthalpy (formation enthalpy and heat capacities at constant pressure) come from Refs.[46–54].

The excess enthalpy is calculated from activity coefficient model

$$h_{\mathrm{i}}^{\mathrm{ex}} = -R.T^2.\frac{\partial \ln(\gamma_{\mathrm{i}}(T, P, x_i))}{\partial T} \tag{16}$$

where h_i^{ex} is the excess enthalpy of compound i (in J mol^{-1}), R is the gas constant (in J mol^{-1} K^{-1}), T is the temperature (in K), γ_{i} is the activity coefficient (–), P is the pressure (in Pa), and x_{i} is the molar fraction of compound i in liquid phase (–).

Results

The first simulation was carried out to validate the use of Pitzer model to calculate activity coefficients. Indeed, the calculation of this thermodynamic property is central for the resolution of the system of equations because of the nonideality of salt solutions. Then, we used the model to simulate the evaporite sequence of artificial salt water.

Validation of the activity coefficient model

Activity Coefficients of Seawater. The activity coefficients of major seawater components have been measured by several workers. We have compared the simulated values with the experimental results that come from Refs. [55–61]. The composition of artificial seawater studied is presented in Table 7.

In Table 8, modeled values of ionic activity coefficients and mean activity coefficients are compared with experimental values at 298.15 K and atmospheric pressure.

Deviations between the calculated results and the experimental data are presented in Table 9. The predicted values are mainly in very good agreement with the measurements. The minimum deviation is for the chloride: 2.1%. The maximum deviation is for the magnesium: 34%. This last deviation is significant but lower compared to the result of Whitfield.[55]

Table 8. Ionic and Mean Activity Coefficients in Seawater (T = 298.15 K and S = 35%)

	Component							
Reference	Na^+	Mg^{2+}	Ca^{2+}	K^+	Cl^-	$SO_4{}^{2-}$	NaCl	Na_2SO_4
Whitfield[55]	0.643	0.222	0.199	0.600	0.69	0.120	–	–
This article	0.651	0.237	0.222	0.608	0.694	0.122	0.672	0.373
Experimental	0.67[a]	0.36[b]	0.24[c]	0.61[d]	0.68[e]	0.11[f]	0.672 ± 0.007[e]	0.378 ± 0.016[f]

[a]From Platford.[58]
[b]From Thompson.[59]
[c]From Thompson and Ross.[60]
[d]From Manglesdorf and Wilson.[61]
[e]From Platford.[56]
[f]From Platford and Dafoe.[57]

Table 10. Artificial Seawater Composition[62]

Component	Molality (mol kg^{-1} d'H_2O)
NaCl	0.428
$MgCl_2$	0.0542
Na_2SO_4	0.0181
$CaSO_4$	0.0099
KCl	0.0091
$NaHCO_3$	0.0012
KBr	0.0008
$CaCl_2$	0.0006

Solubility of Gypsum in Concentrated Seawater. Besides, the solubility of different salts has been compared with experimental data coming from Linke.[62] Here, we present the results of gypsum $CaSO_4{\cdot}2H_2O_{(s)}$ solubility vs. the concentration of an artificial seawater. This salt is an interesting case due to its particular behavior. The composition of the artificial seawater studied is given in Table 10. In Figure 2, the concentration factor is the quotient of the studied solution concentrations divided by the seawater concentrations. The study of the $CaSO_4{\cdot}2H_2O_{(s)}$ solubility in a multicomponent electrolytic system like concentrated seawater at 303.15 K gives a mean relative average deviation of 6% (see Figure 2). The predicted results are in good agreement with the experimental data.

Validation of the dynamic model: evaporite sequence

Our literature review on this topic has showed that very few experimental data in dynamic state have been published. To validate the model in dynamic state, we studied the evaporite sequence of seawater. The composition of artificial seawater studied is presented in Table 10.

According to Gornitz[63] and Warren,[64] the order of salts precipitation at ambient temperature is the following:

Calcite $CaCO_{3(s)}$, Gypsum $CaSO_4{\cdot}2H_2O_{(s)}$, Halite $NaCl_{(s)}$, Sylvite $KCl_{(s)}$. Gornitz[63] indicates that other salts can precipitate at the end of the evaporite sequence, but he does not clearly define these salts.

The evaporite sequence predicted by the model at 298.15 K is the following:

Calcite $CaCO_{3(s)}$, Gypsum $CaSO_4{\cdot}2H_2O_{(s)}$, Halite $NaCl_{(s)}$, Sylvite $KCl_{(s)}$. So, the modeled results are in excellent agreement with experimental and bibliographic data reported in Gornitz[63] and Warren.[64] Besides, the model predicts the precipitation of Anhydrite $CaSO_{4(s)}$ at the end of the evaporite sequence.

Table 11. Initial Apparent Composition

Component	Molality (mol $kg^{-1}H_2O$)
NaCl	1.0
$MgCl_2$	1.0
Na_2SO_4	0.1
KCl	0.1
$CaSO_4$	0.01
$NaHCO_3$	0.002

Table 12. Parameters of the Simulation

Parameter	Value	Unit
Initial temperature	293.15	K
Set point temperature	320.15	K
Initial heat	20,000	W
Initial mass of solution	4.0	kg
Evaporation area	0.044	m^2
Velocity of the air above the vessel	4.0	m s^{-1}
Relative humidity of the air above the vessel	80	%

Simulation of artificial salt water evaporite sequence

The model developed can simulate a salt production process. A purpose of this study is the controlled production of salts and salt waters concentrated in minerals of interest (like magnesium or calcium) using salt spring water as raw material.

To produce characteristic salts with known and fixed composition, we first have to determine the evaporite sequence (the order of salt precipitations), which can depend on temperature.

Figure 1 shows the schematic process. The reactor is filled with salt water. In the batch stirred tank reactor, the solution is heated by constant heat. When the process temperature is equal to the set-point temperature, the system becomes isotherm and the heat required to maintain the solution at constant temperature is determined. With the evaporation of water, the solution is concentrated. Salts precipitation occurs when the solution is saturated by solutes.

Input Parameters. The feed of the reactor is a solution containing classical compounds of natural salt water. The initial apparent composition is given in Table 11. The parameters fixed by the user are given in Table 12.

Evaporite Sequence. The evaporite sequence of the solution with the composition given in Table 11 is the following:

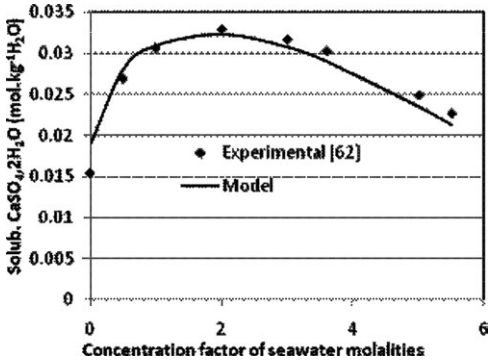

Figure 2. Solubility of gypsum $CaSO_4{\cdot}2H_2O$ in seawater at 303.15 K vs. factor concentration of solution.

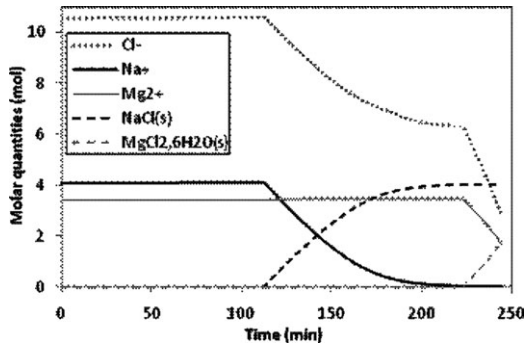

Figure 3. Chloride, sodium, magnesium, halite $NaCl_{(s)}$, and bischofite $MgCl_2{\cdot}6H_2O_{(s)}$ molar quantities vs. time.

Calcite $CaCO_{3(s)}$, *Anhydrite* $CaSO_{4(s)}$, *Halite* $NaCl_{(s)}$, *Sylvite* $KCl_{(s)}$, *Bischofite* $MgCl_2{\cdot}6H_2O_{(s)}$, *Antarcticite* $CaCl_2{\cdot}6H_2O_{(s)}$. Figure 3 shows the molar quantity variations of chloride, sodium, magnesium, halite $NaCl_{(s)}$, and bischofite $MgCl_2{\cdot}6H_2O_{(s)}$. Figure 4 shows the molar quantity variations of potassium and sylvite $KCl_{(s)}$. In Figures 3 and 4, we can see precipitations of halite $NaCl_{(s)}$, sylvite $KCl_{(s)}$, and bischofite $MgCl_2{\cdot}6H_2O_{(s)}$. The precipitation of halite $NaCl_{(s)}$ starts when the time is equal to 120 min. Indeed, the amount of $NaCl_{(s)}$ increases, whereas the amounts of sodium and chloride ions in aqueous solution decrease. The precipitation of sylvite $KCl_{(s)}$ starts at 170 min. The precipitation of bischofite $MgCl_2{\cdot}6H_2O_{(s)}$ starts at 230 min. From this time on, the amount of $MgCl_2{\cdot}6H_2O_{(s)}$ increases, whereas the amounts of magnesium and chloride ions in aqueous solution decrease. Besides, we can see that the model predicts the dissolution of $KCl_{(s)}$ when $MgCl_2{\cdot}6H_2O_{(s)}$ precipitates.

Experimentally, molality will be a composition variable easily accessible. So, we present in Figure 5 the variations of chloride, sodium and magnesium molalities. We can deduce from curve variations the precipitation of halite $NaCl_{(s)}$ and bischofite $MgCl_2{\cdot}6H_2O_{(s)}$. Indeed, we can see variations: on chloride and sodium molality curves at 120 min when $NaCl_{(s)}$ precipitates; and on chloride and magnesium molality curves when $MgCl_2{\cdot}6H_2O_{(s)}$ precipitates at 230 min. It must be emphasized that the precipitation of a salt does not imply the decrease of the molality of anion and cation concerned. This observation is due to the competitive phenomena between evaporation of water and salt precipitation.

Conclusions

A general model was developed to simulate in dynamic state, the behavior of aqueous solution involving liquid, solid, and vapor phases. It is based on the simultaneous resolution of equilibrium equations, mass and energy balances, and electroneutrality and evaporation equations. The resolution method used is Gear's method.

Modeled values of activity coefficients, solubility, and evaporite sequence have been compared with experimental data to validate the equations, the thermodynamic models used, and the general model. The results obtained are satisfactory.

One of the model purposes is the simulation of a controlled-salt production process. To check and validate the simulation results, we will carry out further experiments.

In conclusion, the developed model is a suitable and practical tool for the simulation of salt water behavior.

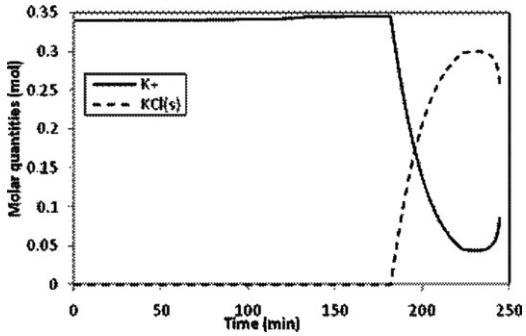

Figure 4. Potassium and sylvite $KCl_{(s)}$ molar quantities vs. time.

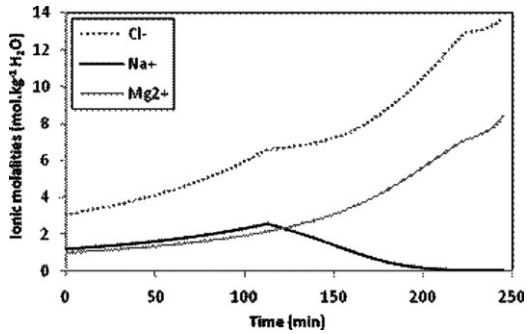

Figure 5. Chloride, sodium and magnesium molalities vs. time.

Notation

a = activity
A = evaporation area of the vessel, m^2
b = number of basic elements
D = dielectric constant, $C^2\ J^{-1}\ m^{-1}$
d_0 = density of water, kg m^{-3}
e = electronic charge, C
f^0 = fugacity of the pure compound, Pa
h^{ex}, h^{id} = excess and ideal enthalpies, J mol^{-1}
h_l, h_c, H_v = liquid, solid (crystal), and vapor enthalpies, J mol^{-1}
H_w = Henry's constant in water, Pa
I = ionic strength, mol kg^{-1}
k = Boltzmann's constant, J K^{-1}
m = molality, mol kg^{-1} H_2O
mK = thermodynamic equilibrium constant
n = molar quantity, mol
N_A = Avogadro's number, mol^{-1}
Q = heat, W
RH = relative humidity
t = time, s
T = temperature, K
U = charge, mol
V = evaporation flow, mol s^{-1}
vel = air velocity, m s^{-1}
x = molar fraction (liquid phase)
y = molar fraction (gas phase)
y_a = molar fraction in the air
z = ionic charge
β, C^Φ, Φ, θ, Ψ, λ, ζ = Pitzer model parameters
ΔH_{LV} = latent heat of vaporization, (J mol^{-1})
γ = activity coefficient
ν = stoichiometric coefficient
Φ = fugacity coefficient

Literature Cited

1. Asdrubali F. A scale model to evaluate water evaporation from indoor swimming pools. *Energy Build*. 2009;41:311–319.
2. Antia HM. *Numerical Methods for Scientists and Engineers*. Boston, Basel, Berlin: Birkhäuser Verlag, 2002.
3. Liddell KN. Thermodynamic models for liquid–liquid extraction of electrolytes. *Hydrometallurgy*. 2005;76:181–192.
4. Ben Gaïda L, Gros J-B, Dussap CG. Activity coefficients of concentrated strong and weak electrolytes by a hydration equilibrium and group contribution model. *Fluid Phase Equilib*. 2010;289:40–48.
5. Lin C-L, Tseng H-C, Lee L-S. A three-characteristic-parameter correlation model for strong electrolyte solutions. *Fluid Phase Equilib*. 1998;15:169–185.
6. Kikic I, Fermeglia M, Rasmussen P. UNIFAC prediction of vapor–liquid equilibria in mixed solvent–salt systems. *Chem Eng Sci*. 1991;46:2775–2780.
7. Chen CC, Britt HI, Boston JF, Evans LB. Local composition models for excess Gibbs energy of electrolyte systems. *AIChE J*. 1982;28:588–596.

8. Lu X, Maurer G. Model for describing activity coefficients in mixed electrolyte aqueous solutions. *AIChE J*. 1993;39:1527–1538.
9. Nicolaisen H, Rasmussen P, Sorensen JM. Correlation and prediction of mineral solubilities in the reciprocal salt system (Na^+, K^+) (Cl^-, SO_4^{2-})–H_2O at 0–100°C. *Chem Eng Sci*. 1993;48:3149–3158.
10. Zemaitis JF, Clark DM, Rafal M, Scrivner NC. *Handbook of Aqueous Electrolyte Thermodynamics*. New-York: AIChE, 1986.
11. Achard C, Dussap CG, Gros JB. Prediction of pH in complex aqueous mixtures using a group contribution method. *AIChE J*. 1994;40: 1210–1222.
12. Gros J-B, Dussap CG. Estimation of equilibrium properties in formulation or processing of liquid foods. *Food Chem*. 2003;82:41–49.
13. Meissner HP, Tester JW. Activity coefficients of strong electrolytes in aqueous solutions. *Ind Eng Chem Process Des Dev*. 1972;11:128–133.
14. Bromley LA. Thermodynamic properties of strong electrolytes in aqueous solutions. *AIChE J*. 1973;19:313–320.
15. Pitzer KS. Thermodynamics of electrolytes. I. Theoretical basis and general equation. *J Phys Chem*. 1973;77:268–277.
16. Millero FJ, Pierrot D. A chemical model for natural waters. *Aquat Geochem*. 1998;4:153–199.
17. Marliacy P, Hubert N, Schuffenecker L, Solimando R. Use of Pitzer's model to calculate thermodynamic properties of aqueous electrolyte solutions of Na_2SO_4 + NaCl between 273.15 and 373.15 K. *Fluid Phase Equilib*. 1998;148:95–106.
18. Pabalan RT, Pitzer KS. Thermodynamics of NaOH(aq) in hydrothermal solutions. *Geochim Cosmochim Acta*. 1987;51:829–837.
19. Pitzer KS, Peiper JC, Busey RH. Thermodynamic properties of aqueous sodium chloride solutions. *J Phys Chem Ref Data*. 1984;13:1–102.
20. Spencer RJ, Moller N, Weare JH,The prediction of mineral solubilities in natural waters: A chemical equilibrium model for the Na–K–Ca–Mg–Cl–SO_4–H_2O system at temperatures below 25°C. *Geochim Cosmochim Acta*. 1990;54:575–590.
21. He S, Morse JW. The carbonic acid system and calcite solubility in aqueous Na–K–Ca–Mg–Cl–SO_4 solutions from 0 to 90°C. *Geochim Cosmochim Acta* 1993;57:3533–3555.
22. Peiper JC, Pitzer KS. Thermodynamics of aqueous carbonate solutions including mixtures of sodium carbonate, bicarbonate and chloride. *J Chem Thermodyn*. 1982;14:613–638.
23. Silvester LF, Pitzer KS. Thermodynamics of electrolytes, X. Enthalpy and the effect of temperature on the activity coefficients. *J Solution Chem*. 1978;7:327–337.
24. Criss C, Millero FJ. Modeling the heat capacities of aqueous 1-1 electrolyte solutions with Pitzer's equations. *J Phys Chem*. 1996;9:1288–1294.
25. Pitzer KS, Mayorga G. Thermodynamics of electrolytes. II. Activity and osmotic coefficients with one or both ions univalent. *J Phys Chem*. 1973;77:2300–2308.
26. Holmes HF, Mesmer RE. Thermodynamic properties of aqueous solutions of the alkali metal chlorides to 25°C. *J Phys Chem*. 1983;87:1242–1255.
27. Marion GM, Farren RE. Mineral solubilities in the Na–K–Mg–Ca–Cl–SO_4–H_2O system: a re-evaluation of the sulfate chemistry in the Spencer-Moller-Weare model. *Geochim Cosmochim Acta* 1999;63:1305–1318.
28. De Lima MCP, Pitzer KS. Thermodynamics of saturated electrolyte mixtures of NaCl with Na_2SO_4 and $MgCl_2$. *J Solution Chem*. 1983;12:187–199.
29. Holmes HF, Busey RH, Simonson JM, Mesmer RE, Archer DG, Wood RH. The enthalpy of dilution of HCl(aq) to 648 K and 40 MPa, thermodynamic properties. *J Chem Thermodyn*. 1987;19:863–890.
30. Pierrot D, Millero FJ, Roy LN, Roy RN, Doneski A, Niederschmidt J. The activity coefficients of HCl in HCl–Na_2SO_4 solutions from 0 to 50°C and ionic strengths up to 6 molal. *J Solution Chem*. 1997;26:31–45.
31. Campbell DM, Millero FJ, Roy R, Roy L, Lawson M, Vogel KM, Moore CP. The standard potential for the hydrogen-silver, silver chloride electrode in synthetic seawater. *Mar Chem*. 1993;44:221–233.
32. Moller N. The prediction of mineral solubilities in natural waters: a chemical equilibrium model for the Na–Ca–Cl–SO_4–H_2O system, to high temperature and concentration. *Geochim Cosmochim Acta*. 1988;52:821–837.
33. Greenberg JP, Moller N. The prediction of mineral solubilities in natural waters: a chemical equilibrium model for the Na–K–Ca–Cl–SO_4–H_2O system to high concentration from 0 to 250°C. *Geochim Cosmochim Acta*. 1989;53:2503–2518.
34. Harvie CE, Moller N, Weare JH. The prediction of mineral solubilities in natural waters: the Na–K–Mg–Ca–H–Cl–SO_4–OH–HCO_3–CO_3–CO_2–H_2O system to high ionic strengths at 25°C. *Geochim Cosmochim Acta*. 1984;48:723–751.
35. Thurmond V, Millero FJ. Ionization of carbonic acid in sodium chloride solutions. *J Solution Chem*. 1982;11:447–456.
36. Roy RN, Gibbons JJ, Trower JK, Lee GA, Hartley JJ, Mack JG. The ionization constant of carbonic acid in solutions of sodium chloride from e.m.f. measurements at 278.15, 298.15, and 318.15 K. *J Chem Thermodyn*. 1982;14:473–482.
37. Marion GM. Carbonate mineral solubility at low temperatures in the Na–K–Mg–Ca–H–Cl–SO_4–OH–HCO_3–CO_3–CO_2–H_2O system. *Geochim Cosmochim Acta*. 2001;65:1883–1896.
38. Roy RN, Gibbons JJ, Wood MD, Williams RW, Peiper JC, Pitzer KS. The first ionization of carbonic acid in aqueous solutions of potassium chloride including the activity coefficients of potassium bicarbonate. *J Chem Thermodyn*. 1983;15:37–47.
39. Risacher F, Fritz B. Estimation des variations en fonction de la température des produits de solubilité des principaux sels des milieux évaporitiques. *Sci Geol*. 1984;37:229–237.
40. Johnson JW, Oelkers EH, Helgeson HC. SUPCRT92: a software package for calculating the standard molal thermodynamic properties of minerals, gases, aqueous species, and reactions from 1 to 5000 bar and 0 to 1000°C. *Comput Geosci*. 1992;18:899–947.
41. Jimenez YP, Taboada ME, Galleguillos HR. Solid–liquid equilibrium of K_2SO_4 in solvent mixtures at different temperatures. *Fluid Phase Equilib*. 2009;284:114–117.
42. Plummer LN, Parkhurst DL, Fleming GW, Dunkle SA. A computer program incorporating Pitzer's equations for calculation of geochemical reactions in brines. U.S. Geological Survey Water-Resources Investigations.1988:88–4153.
43. Marshall WL, Slusher R. Thermodynamics of calcium sulphate dihydrate in aqueous sodium chloride solutions, 0–110°C. *J Phys Chem*. 1966;70:4015–4027.
44. Stull DR. Vapor pressure of pure substances organic compounds, *Ind Eng Chem*. 1947;39:517–540.
45. Yaws CL, Hopper JR, Wang X, Rathinsamy AK, Pike RW. Calculating solubility and Henry's law constants for gases in water. *Chem Eng*.1999;106:102–105.
46. Patnaik P. *Handbook of Inorganic Chemicals*. New York: McGraw-Hill, 2002.
47. Mullin JW. *Crystallization*. Butterworth-Heinemann: Oxford, 2001.
48. Königsberger E, Königsberger L-C, Gamsjäger H. Low-temperature thermodynamic model for the system Na_2CO_3–$MgCO_3$–$CaCO_3$–H_2O. *Geochim Cosmochim Acta*. 1999;63:3105–3119.
49. Perry RH, Green DW. *Perry's Chemical Engineers' Handbook*. New York: McGraw-Hill, 1997.
50. Knacke O, Kubaschewski O, Hesselmann K. *Thermochemical Properties of Inorganic Substances*. Berlin: Springer-Verlag, 1991.
51. Pitzer KS. *Activity Coefficients in Electrolyte Solutions*, 2nd ed. In: KS Pitzer editor. Boca Raton, FL: CRC Press, 1991.
52. Raju KUG, Atkinson G. The thermodynamics of scale mineral solubilities. 3. Calcium sulfate in aqueous NaCl. *J Chem Eng Data*. 1990;35:361–367.
53. Plummer LN, Busenberg E. The solubilities of calcite, aragonite and vaterite in CO_2–H_2O solutions between 0 and 90°C, and an evaluation of the aqueous model for the system $CaCO_3$–CO_2–H_2O. *Geochim Cosmochim Acta*. 1982;46:1011–1040.
54. Helgeson HC, Kirkham DH, Flowers GC. Theoretical prediction of the thermodynamic behavior of aqueous electrolytes. IV. Calculation of activity coefficients, osmotic coefficients and apparent molal and standard and relative partial molal properties to 600°C and 5 kb. *Am J Sci*. 1981;281:1249–1516.
55. Whitfield M. *Activity Coefficients in Natural Waters*. In: Pytkowicz RM editor, Boca Raton, FL: CRC Press, 1979.
56. Platford RF. The activity coefficient of sodium chloride in seawater. *J Mar Res*. 1965;23:55–62.
57. Platford RF, Dafoe T. The activity coefficient of sodium sulfate in seawater. *J Mar Res*. 1965;23:63–68.
58. Platford RF. Activity coefficient of the sodium ion in sea water. *J Fish Res Bd Canada*. 1965;22:885–889.
59. Thompson ME. Magnesium in sea water: an electrode measurement. *Science*. 1966;153:866–867.
60. Thompson ME, Ross JW. Calcium in sea water by electrode measurement. *Science*. 1966;154:1643–1644.
61. Mangelsdorf PC, Wilson TRS. Difference chromatography of seawater. *J Phys Chem*. 1971;75:1418–1425.
62. Linke WF. *Solubilities of Inorganic and Metal Organic Compounds*, 4th ed. Washington: American Chemical Society, 1958.

63. Gornitz V. *Encyclopedia of Paleoclimatology and Ancient Environments*, Dordrecht: Springer, 2009.
64. Warren JK. *Evaporites: Sediments, Resources and Hydrocarbons*. Berlin: Springer, 2006.

Appendix: Additional equations of Pitzer model

The additional equations of Pitzer model are detailed in this appendix.[10,16,17]

$$F = f^{\gamma} + \sum_{c=1}^{n_c}\sum_{a=1}^{n_a} m_c.m_a.B'_{ca} + \sum_{c=1}^{n_c-1}\sum_{c'=2}^{n_c} m_c.m_{c'}\Phi'_{cc'} + \sum_{a=1}^{n_a-1}\sum_{a'=2}^{n_a} m_a.m_{a'}.\Phi'_{cc'} \tag{A1}$$

For 1-1, 2-1, 1-2, 3-1, 4-1, and 5-1 electrolytes

$$B_{ca} = \beta_{0_{ca}} + \frac{2.\beta_{1_{ca}}}{\alpha_1^2.I}.[1-(1+\alpha_1.\sqrt{I}).\exp(-\alpha_1.\sqrt{I})] \tag{A2}$$

$$B'_{ca} = -\frac{2}{\alpha_1^2.I^2}.\left[\beta_{1_{ij}}.\left(1-\left(1+\alpha_1.\sqrt{I}+\frac{\alpha_1^2.I}{2}\right).\exp(-\alpha_1.\sqrt{I})\right)\right] \tag{A3}$$

For 2-2 electrolytes

$$B_{ca} = \beta_{0_{ca}} + \frac{2.\beta_{1_{ca}}}{\alpha_2^2.I}.[1-(1+\alpha_2.\sqrt{I}).\exp(-\alpha_2.\sqrt{I}] + \frac{2.\beta_{2_{ca}}}{\alpha_3^2.I}.[1-(\alpha_3.\sqrt{I}).\exp(-\alpha_3.\sqrt{I})] \tag{A4}$$

$$B'_{ca} = -\frac{2.\beta_{1_{ij}}}{\alpha_2^2.I^2}.\left[1-\left(1+\alpha_2.\sqrt{I}+\frac{\alpha_2^2.I}{2}\right).\exp(-\alpha_2.\sqrt{I})\right] - \frac{2.\beta_{2_{ij}}}{\alpha_3^2I^2}.\left[1-\left(1+\alpha_3.\sqrt{I}+\frac{\alpha_3^2.I}{2}\right).\exp(-\alpha_3.\sqrt{I})\right] \tag{A5}$$

with $\alpha_1 = 2$, $\alpha_2 = 1.4$, $\alpha_3 = 12$.

$$C_{ca} = \frac{C^{\Phi}}{2.\sqrt{|z_c.z_a|}} \tag{A6}$$

$$\Phi_{ij} = \theta_{ij} + {}^{E}\theta_{ij} \tag{A7}$$

Parameters ${}^{E}\theta_{ij}$ are assumed null.

$$f^{\gamma} = -A_{\Phi}.\left[\frac{\sqrt{I}}{1+b.\sqrt{I}} + \frac{2}{b}.\ln(1+b.\sqrt{I})\right] \tag{A8}$$

with $b = 1.2$.
A_{Φ} is the Debye-Huckel constant

$$A_{\Phi} = \frac{1}{3}.\left(\frac{e}{\sqrt{D.k.T}}\right)^3.\sqrt{2.\pi.d_0.N_A} \tag{A9}$$

Manuscript received Sep. 26, 2011, and revision received Jan. 13, 2012.